

Nitroxide-radicals–modified gold nanorods for in vivo CT/MRI-guided photothermal cancer therapy

Luyao Xia^{1,2}Chao Zhang¹Min Li¹Kaiyu Wang¹Yushan Wang¹Peipei Xu¹Yong Hu²

¹Department of Hematology, Drum Tower Hospital, School of Medicine, Nanjing University, Nanjing, Jiangsu, 210093, People's Republic of China;

²College of Engineering and Applied Science, Nanjing University, Nanjing, Jiangsu, 210093, People's Republic of China

Purpose: This article presents a report of the synthesis, characterization, and biomedical application of nitroxide-radicals–modified gold nanorods (Au-TEMPO NRs) for imaging-guided photothermal cancer therapy.

Patients and methods: Au nanorods were synthesized through seed-mediated growth method, 4-Amino-TEMPO was added and the reaction proceeded under magnetic stirring.

Results: With a mean length of 39.2 nm and an average aspect ratio of approximately 3.85, Au-TEMPO NRs showed good photothermal ability when they were irradiated by 808-nm laser. Au-TEMPO NRs could be stored in PBS for more than 1 month, showed no cytotoxicity against both tumor and normal cells at a concentration of up to 3 mg/mL, and functioned as a dual-mode contrast agent for CT/magnetic resonance (MR) imaging in vitro and in vivo, due to their high X-ray attenuation of Au and good r1 relaxivity of nitroxide radicals. Further, they had a long retention time (~4 hours) in the main organs, which enabled a long CT/MR imaging time window for diagnosis. Bio-distribution results revealed that these Au-TEMPO NRs passively aggregated in the liver and spleen. After irradiation by 808-nm laser, Au-TEMPO NRs could ablate the solid tumor in 4T1 tumor-bearing mice, which implied they were a potential theranostic agent for dual-mode imaging and photothermal cancer therapy.

Conclusion: This type of Au-TEMPO NRs with the abilities of CT/MR imaging and photothermal therapy, can play an active role in imaging-guided photothermal cancer therapy.

Keywords: PTT, Au NRs, TEMPO, computed tomography, magnetic resonance imaging

Introduction

Molecular imaging techniques have undergone rapid growth in recent years because they can provide more specific physiological and pathological information as compared to traditional anatomical imaging methods.^{1,2} Several imaging modalities have been developed and widely used for the clinical diagnosis and treatment of cancer such as CT and magnetic resonance imaging (MRI).^{3–5} CT imaging is one of the most effective and irreplaceable imaging methods in clinical diagnosis, providing anatomic structure and functional information because of its high-density resolution and rapid sweep speed.⁶ However, there is insufficient contrast between soft tissues and organs due to the inherent extinction ability of X-rays. In contrast, although MRI has good spatial resolution and high sensitivity to tissue structures, it needs a longer scanning time and requires contrast agents to have a longer half-decay time and better stability.⁷ To address these limitations, many studies have reported on contrast agents that can improve the diagnostic imaging quality in these modalities.^{8–10}

Iodinated ionic or nonionic agents are clinically used in CT measurement due to their low cost and high X-ray absorption; however, these small molecules were reported to have a risk of infectious diseases and nephrotoxicity after injection.¹¹ Gd(III)-^{4,12,13} or Mn(II)-^{14–16}

Correspondence: Peipei Xu
Department of Hematology, The
Affiliated Drum Tower Hospital of
Nanjing University Medical School,
Nanjing University, Nanjing 210008,
People's Republic of China
Tel/fax +86 25 8310 5211
Email xu_peipei0618@163.com

Yong Hu
College of Engineering and Applied
Science, Nanjing University, 22 Hankou
Road, Nanjing 210093, People's Republic
of China
Email huyong@nju.edu.cn

based T1-weighted MR contrast agents and superparamagnetic iron oxide nanoparticles (NPs)-based T2-weighted MR contrast agents are widely used and well tolerated by most patients.^{17,18} Because each imaging modality has its own advantages and limitations, multi-mode – especially dual-mode – imaging contrast agents, combining CT and MR imaging abilities, have received much research interest in this field to obtain more comprehensive and accurate diagnostic information.

To successfully obtain dual-mode CT/MRI contrast agents, multicomponent NPs – integrating both MRI and CT imaging materials – have proved to be unique candidates as main enablers of imaging agents. Gd(III)-Au NPs,^{4,13} Fe₃O₄-AuNPs,¹⁹ and Fe-Pt NPs²⁰ have been used for CT/MR dual-mode imaging. However, metal-based ions, such as gadolinium, have been thought to be responsible for some adverse reactions, including nephrogenic systemic fibrosis.²¹ Furthermore, these agents are always prepared through complicated processes, and the synthesis procedure is time consuming. Thus, it remains a challenge to simplify the preparatory steps and obtain more accurate pathological images for the diagnosis and treatment of miscellaneous diseases with better biocompatibility.²²

Recently, Au NPs have been widely applied as theranostic agents that combine diagnostic and therapeutic abilities because of their low cytotoxicity, high biocompatibility, and strong X-ray-attenuating potency.²³ Furthermore, due to their easy functional surface, the targeting ligands are easily conjugated to the surface of these Au NPs to obtain nanomedicines, which can be applied in targeted cancer treatment.^{24,25} By conjugating a tumor-homing peptide to Au nanorods, breast cancer precision medicine was successfully obtained that could enhance the accumulation of Au nanorods in tumor tissue and improve the cancer-killing efficacy.²⁶ However, metal-free organic nitroxide radicals have been reported to be promising T₁ contrast agents owing to their superparamagnetic performance, high ¹H water relaxivities (*R*₁), and long in vivo-circulation time.^{27,28} Nitroxide-radicals-modified materials have been successfully applied as T₁ contrast agents to study the redox status in tumors.^{29,30} Therefore, in the present study, nitroxide-radicals-conjugated Au nanorods (Au-TEMPO NRs) were synthesized via a simple bio-conjugation method.^{31,32} These Au-TEMPO NRs showed excellent CT imaging ability and remarkable MRI-enhanced contrast ability due to the strong X-ray-attenuating potency of Au and the high *R*₁ from nitroxide radicals. Furthermore, Au NRs are supposed to be good photothermal materials and have been widely used to ablate tumor tissues with laser irradiation. We are convinced that this type of Au-TEMPO NR, which integrate the abilities of CT/MR imaging and

photothermal therapy abilities, can play an active role in imaging-guided photothermal cancer therapy.

Methods

Materials

Hexadecyltrimethylammonium bromide (CTAB), chloroauric acid (HAuCl₄), sodium borohydride (NaBH₄), silver nitrate (AgNO₃), ascorbic acid, 1-ethyl-3-(3-dimethylaminopropyl)-carbodiimide (EDC), and N-hydroxysuccinimide (NHS) were purchased from Sigma-Aldrich (St Louis, MO, USA). Moreover, 4-amino-2,2,6,6-tetramethylpiperidine-N-oxide (4-Amino-TEMPO) and HOOC-mPEG-SH (MW ~2 kDa) were purchased from Laysan Bio (Arab, AL, USA). Cells from the murine breast tumor cell line 4T1 and human umbilical vein endothelial cells (HUVECs) were purchased from the Shanghai Institute of Cell Biology (Shanghai, China). PBS and all other aqueous solutions were prepared with ultrapure water obtained from a Millipore ultrapure water system (Billerica, MA, USA).

Synthesis of Au NRs

Au nanorods (Au NRs) were synthesized through a seed-mediated growth method as previously reported.³³ The seed solution was prepared by adding 100 μL of 0.01 M HAuCl₄ and 500 μL of 0.01 M NaBH₄ to CTAB solution (8.0 mL, 0.05 M). After vigorous stirring, the solution turned brownish yellow and was kept at 25°C for 2 hours. The growth solution was prepared by adding 165 μL of 0.01 M HAuCl₄ to CTAB solution (4.5 mL, 0.10 M); then 30 μL of 0.01 M AgNO₃ and 0.03 mL of 0.01 M ascorbic acid were added and the color of this solution changed from dark yellow to colorless after gentle shaking for a few seconds. After that, 0.04 mL of this seed solution was added to the growth solution and the growth solution was kept at 37.5°C overnight. Finally, this reaction solution was centrifuged and washed with distilled water thrice to obtain the purified Au NRs.

Conjugation of 4-amino-TEMPO to Au NRs

Au NRs were dispersed in 5 mL ultrapure water and reacted with excessive HOOC-mPEG-SH (MW ~2 kDa) overnight under magnetic stirring. Then, 0.5 mg EDC and 0.3 mg NHS were added to activate the carboxyl group for approximately 2 hours. Next, 1.0 mg 4-Amino-TEMPO was added and the reaction proceeded under magnetic stirring at room temperature for 12 hours. The final product of Au-TEMPO NRs was centrifuged and re-dispersed in ultrapure water at different concentrations.

Characterization

The morphology of Au-TEMPO NRs was investigated by high-resolution transmission electron microscopy (TEM; JEM-200CX). Surface plasma resonance properties were investigated by a UV-Vis-NIR spectrophotometer (Shimadzu UV-3600). The surface element composition was investigated by X-ray photoelectron spectroscopy (XPS; PHI 5000 Versa Probe). Magnetic properties were detected via an electron paramagnetic resonance spectrometer (EPR; EMX-10/12).

Cytotoxicity assay (MTT)

The cytotoxicity of Au-TEMPO NRs was tested via an MTT colorimetric assay. Cells of the murine breast tumor cell line 4T1 and HUVECs were seeded at a density of 10^4 cells/well in 96-well plates in 100 μ L DMEM and incubated at 37°C in 5% CO₂ atmosphere for 48 hours. The medium in each well was then replaced with 100 μ L fresh medium containing various concentrations of Au-TEMPO NRs with five replicates. After 12 hours, the medium was discarded, and the cells were washed thrice with PBS, followed by the addition of 20 μ L MTT solution (2.5 mg/mL in PBS) and fresh medium. Cells were further incubated for 4 hours, followed by removal of the culture medium with MTT, and then 200 μ L DMSO was added into each well. The resulting mixture was shaken for 5 minutes at room temperature and absorbance was measured at 490 nm by using an iMark Enzyme mark instrument (Bio-Rad Inc., Hercules, CA, USA) to estimate the cell viability.

Photothermal irradiation

The Au-TEMPO NRs suspension (1,000 μ g/mL) was irradiated for 15 minutes in 24-well plates with an 808-nm laser at a power of 1.13 W/cm² (1.76 cm² laser area) at room temperature, and the suspension temperature was recorded every minute. For the in vitro photothermal experiment of 4T1 cells, the 4T1 cells were first seeded at a density of 10^4 cells/well in 96-well plates in 100 μ L DMEM and incubated at 37°C in 5% CO₂ atmosphere for 48 hours. The medium in each well was then replaced with 100 μ L fresh medium containing various concentrations of the Au-TEMPO NRs, with five replicates. Then, each well was treated with 808-nm laser irradiation for 15 minutes. Finally, the cell viabilities were tested via the MTT colorimetric assay.

In vitro cellular imaging

The 4T1 cells were seeded in a six-well Petri dish at a density of 10^5 cells per well and incubated overnight at 37°C. Thereafter, Au-TEMPO NRs were added into the wells

at different concentrations for 4 hours. Three wells were irradiated for 15 minutes under 808-nm laser. Cells without irradiation treatment were used as the control. Cells were harvested by trypsinization and centrifugation at 800 rpm for 5 minutes. For flow cytometry (FCM) as well as an Annexin V–fluorescein isothiocyanate (FITC) and a propidium iodide (PI) apoptosis detection kit (BD Biosciences) were used according to the manufacturer's protocol. The test was conducted on a BD FACSVerse flow cytometer, and the data were analyzed.

For fluorescence microscope observation, 4T1 cells were stained with a Calcein-AM/PI Kit (BD Biosciences) according to the manufacturer's protocol. Both living and dead cells were observed under excitation at 490 nm, and only dead cells were observed under excitation at 545 nm. The images were processed by Photoshop CS6.

In vitro and in vivo CT imaging study

The CT images were collected by a clinical CT Gemstone spectral 64-Detector CT (Discovery CT 750HD, GE Amer-sham Healthcare System, Milwaukee, WI, USA) at an X-ray voltage of 80 KVp and anode current of 10 mA. A solution of Au-TEMPO NRs and iodixanol with gradient concentration (in respect of Au or I concentration as 95, 188, 375, 750, 1,500, and 3,000 μ g/mL) was added into a 96-well cell culture plate, and deionization water was selected as the control for comparison. Female BALB/c mice (8–10 weeks old, weighing 18–22 g) were used for CT imaging. The 4T1 cells (5×10^6 cells per mouse) were injected subcutaneously into the right armpit of the mice, and experiments were carried out when the tumor volume reached approximately 0.2 cm³. The mice were first anesthetized by an intraperitoneal injection of 10% chloral hydrate (3 mL/kg). A suspension of Au-TEMPO NRs (0.1 mL [Au]=1,000 μ g/mL PBS) was injected into the subcutaneous tumor. CT scans were done at 0 minute, 5 minutes, 30 minutes, 1 hour, 4 hours, and 12 hours post injection. The images were processed with Radiant DICOM Viewer and Photoshop CS6. The animal tests were approved by the institutional ethical committee for animal care in Nanjing University and conducted in accordance with the policy and protocols of the National Ministry of Health.

In vitro and in vivo MRI study

In vitro MR images were collected by a 1.5 T clinical MRI scanner (Nova Dual Philips). Parameters for the image collection included: fast spin echo, repetition time (TR)=580 ms, echo time (TE)=18 ms, and slice thickness=1.1 mm. A suspension of Au-TEMPO NPs (dispersed in gelatin [Au]=95,

188, 375, 750, 1,500, and 3,000 $\mu\text{g/mL}$) was added into a 24-well cell culture plate, and gelatin was selected for comparison. Female BALB/c mice (8–10 weeks old, weighing 18–22 g) were used for *in vivo* imaging. The 4T1 cells (5×10^6 cells per mouse) were injected subcutaneously into the right armpit of the mice 4 weeks before the experiments. The mice were first anesthetized by an intraperitoneal injection of 10% chloral hydrate (3 mL/kg). A suspension of Au-TEMPO NRs (0.1 mL, $[\text{Au}] = 1,000 \mu\text{g/mL}$) dispersed in PBS was injected to the subcutaneous tumor. MR scans were done at 0 minute, 5 minutes, 30 minutes, 1 hour, 4 hours, and 12 hours post injection. *In vivo* T1-weighted MR images of rat were collected by a MicroMRI system (Biospec 7T/20 USR, Bruker). Parameters for the image collection included: fast spin echo, repetition time (TR)=300 ms, echo time (TE)=8.9 ms, and slice thickness=0.7 mm. MR data were analyzed using T1-weighted signal intensity. The images were processed with Radiant DICOM Viewer and Photoshop CS6. The animal tests were approved by the institutional ethics committee for animal care in Nanjing University and conducted in accordance with the policy and protocols of the National Ministry of Health.

In vivo antitumor effect

Female BALB/c mice were administered subcutaneous injections of 4T1 cells (5×10^6 cells per mouse) into the right armpits to acquire 4T1–tumor-bearing mice. After 10 days, the tumor volume reached $\sim 200 \text{ mm}^3$, and these tumor-bearing mice were randomly divided into three groups with eight mice in each group: a PBS group, an Au-TEMPO NRs group, and an Au-TEMPO NRs + Laser group. Each mouse was administered 100 μL sample solution (1 mg/mL Au-TEMPO NRs) via tail-vein injection. After 4 hours, the tumor area was irradiated with an 808-nm laser (1.13 W/cm²) for 10 minutes. The tumor volume and the survival of each mouse were monitored and recorded during the experimental duration.

Histological study

Female BALB/c mice (weighing 18–22 g) were used for *in vivo* bio-distribution studies of the Au-TEMPO NPs. Mice were first anesthetized by intraperitoneal injection of 10% chloral hydrate (3 mL/kg). Then, Au-TEMPO NRs (0.1 mL in PBS solution $[\text{Au}] = 1,000 \mu\text{g/mL}$) were injected via the tail vein. The mice were euthanized at 1, 4, 8, 12, 24, and 48 hours post injection and the heart, liver, spleen, lung, kidney, and blood were extracted. After being weighed, the organs were digested by aqua regia solution overnight, and the Au

content was determined by Inductively Coupled Plasma Optical Emission Spectrometer (Optima 5,300DV).

In order to evaluate potential acute cytotoxicity, the major organs of mice (24/48 hours post injection), such as the heart, liver, spleen, lung, and kidney, were extracted and immobilized in 4% paraformaldehyde for 48 hours. Randomly picked sections from the organs embedded in paraffin were stained with hematoxylin and eosin (H&E) and observed under a light microscope at $\times 100$ magnification.

Results and discussion

Characterization of Au-TEMPO NRs

The seed-mediated growth method was used to synthesize Au NRs. To stabilize the Au NRs thus obtained, they were modified with HOOC-mPEG-SH due to the formation of the Au-S bonds (Figure 1). The 4-Amino-TEMPO was connected to Au NRs through an NHS/EDC-catalyzed $-\text{COOH}/-\text{NH}_2$ condensation reaction. The final product showed good stability and could be stored in water and saline solution for more than 1 month.

The size and the morphology of Au NRs were measured by TEM as shown in Figure 2A. These Au NRs have a mean length of 39.2 nm and their average aspect ratio was approximately 3.85. After the modification of 4-Amino-TEMPO on the surface of Au NRs, the color of the solution changed slightly. The UV-vis absorption curve of 4-Amino-TEMPO and the longitudinal absorption bands of Au NRs and Au-TEMPO NRs were tested with the UV-vis spectrum, as shown in Figure 2C. Clearly, 4-Amino-TEMPO shows absorption at approximately 435 nm that is attributable to the nitroxide free radicals, and no other obvious peak was seen above 480 nm. For Au NRs, two peaks centered at 520/785 nm were observed, in agreement with the reported literature.³⁴ As for Au-TEMPO NRs, there are two characteristic peaks

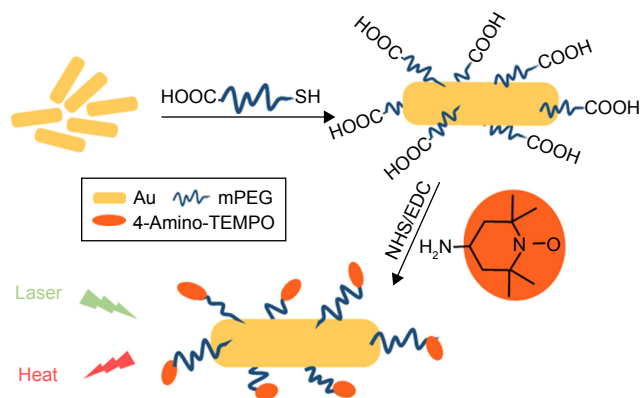


Figure 1 Synthesis of Au-TEMPO NRs.

Abbreviation: Au-TEMPO NRs, nitroxide-radicals–modified gold nanorods.

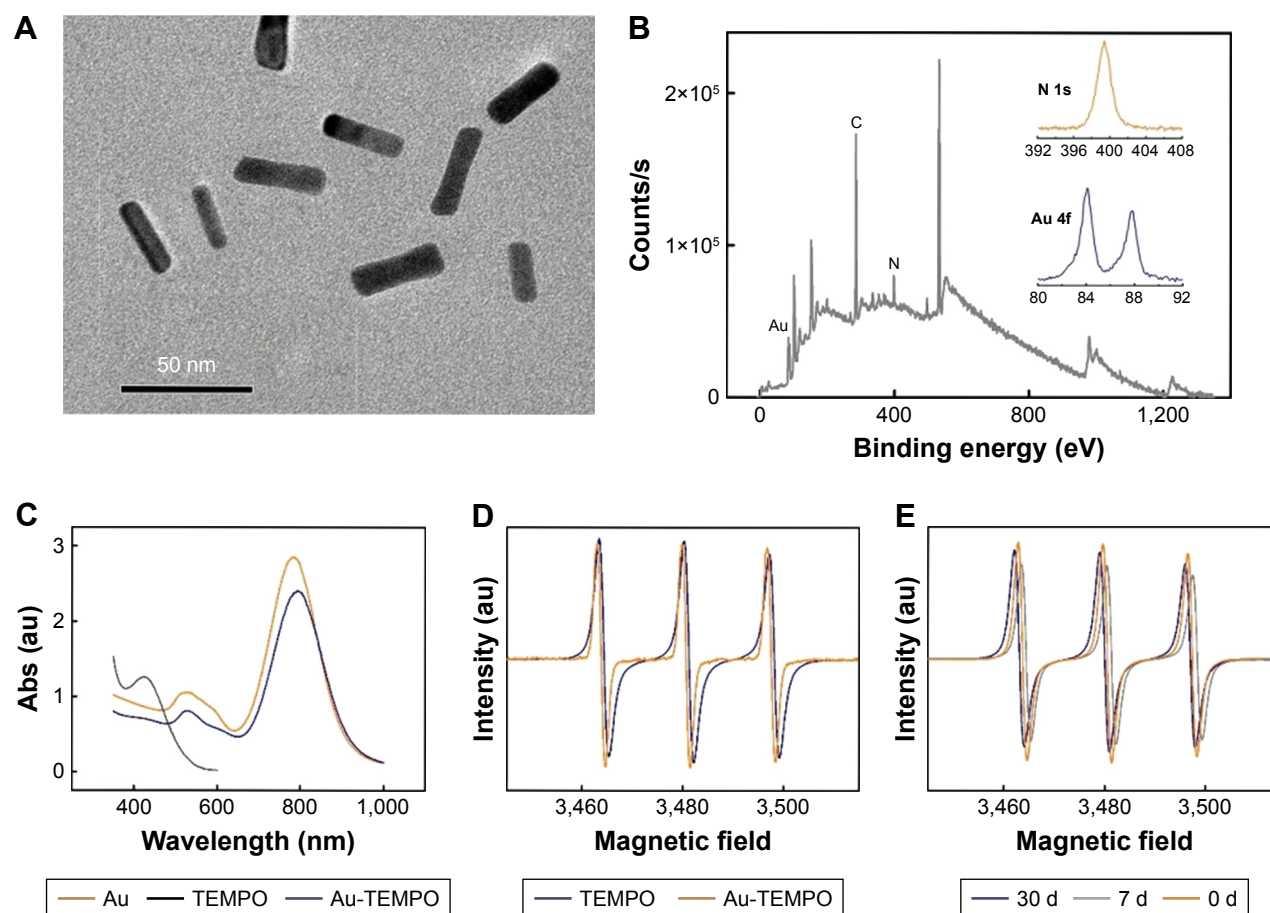


Figure 2 (A) TEM image of Au NRs, (B) XPS spectra of Au-TEMPO NRs. (C) UV-vis absorption spectra of TEMPO, Au NRs, and Au-TEMPO NRs. (D) EPR signals of TEMPO and Au-TEMPO NRs. (E) EPR signal of Au-TEMPO NRs stored in PBS at 0, 7, and 30 days.

Abbreviation: Au-TEMPO NRs, nitroxide-radicals–modified gold nanorods.

at 525/792 nm in the UV-vis spectrum, belonging to the longitudinal and transverse oscillation of surface plasmon bands of Au NRs, with a slight red shift, compared to the original Au NRs. Besides this, a weak absorption peak at 440 nm, attributed to the 4-Amino-TEMPO, is observed. Furthermore, the conjugation of 4-Amino-TEMPO to Au NRs was verified by XPS measurement. Figure 2B reveals the XPS spectrum of Au-TEMPO NRs. Except for the peak of the Au element, the peak of the N element (400 eV) from 4-Amino-TEMPO is clearly observed – confirming the successful conjugation of 4-Amino-TEMPO with Au NRs. Moreover, the surface modification can be confirmed by changes of zeta potential of Au NRs during the synthesis procedure. In Table 1, the zeta-potential of the Au NRs is

Table 1 Zeta-potential of Au NRs, Au-mPEG-COOH NRs, and Au-TEMPO NRs

Sample	Au NRs	Au-mPEG-COOH NRs	Au-TEMPO NRs
Zeta-potential (mV)	38.8±1.4	-24.6±2.3	-6.3±1.8

Abbreviation: Au-TEMPO NRs, nitroxide-radicals–modified gold nanorods.

38.8 mV in the CTAB solution because of the absorption of CTAB. After the modification of HOOC-mPEG-SH, the zeta potential turns negative due to the negative charge of the carboxyl group. The zeta potential eventually increases because the carboxyl of mPEG can react with the amino group of 4-Amino-TEMPO and there are lesser carboxyl groups on the surface of Au-TEMPO NRs.

TEMPO is a type of stable, organic, free radical and is an electron paramagnetic resonance (EPR)-active molecule displaying a triplet curve in the EPR spectrum.³⁵ The presence of TEMPO on the surface of Au-TEMPO NRs was checked by the EPR test. Free 4-Amino-TEMPO has a triplet curve in the EPR spectrum, and Au-TEMPO NRs shows a similar EPR spectrum, further proving that TEMPO was conjugated with Au NRs as we expected (Figure 2D). To be used as diagnostic agents, these Au-TEMPO NRs should be sufficiently stable under normal physiological conditions. Therefore, the stability of these Au-TEMPO NRs, especially the stability of nitroxide radicals, should be tested. To address this concern, periodic EPR tests were

conducted to inspect the stability of Au-TEMPO NRs after being stored in PBS for a long time. Clearly, despite the tiny shifts, no significant decrease or deviation in EPR signals of Au-TEMPO NRs was observed, even in Au-TEMPO NRs stored in PBS for 30 days (Figure 2E). Thus, it is proved that Au-TEMPO NRs are quite stable and can be used as a contrast agent *in vivo*.

Cytotoxic assay of Au-TEMPO NRs

Before the Au-TEMPO NRs can be used as diagnostic agents, their *in vitro* cyto-compatibility should be evaluated. Cells of the murine breast tumor cell line 4T1 and HUVECs were both used to clarify the different cytotoxic effects on cancer cells and normal cells. After these cells were incubated with Au-TEMPO NRs at different concentrations for 12 hours, an MTT assay was carried out to investigate the cytotoxicity. Only a 12.8% reduction in cell viability was observed at the highest Au concentration of 3,000 $\mu\text{g/mL}$ for 4T1 cells (Figure 3A), as was an 8.6% reduction of cell viability for HUVECs (Figure 3B). These results clearly indicated that Au-TEMPO NRs exerted a negligible cytotoxic effect on tumor cells and normal cells even at high concentrations, thereby proving the safety and biocompatibility of Au-TEMPO NRs to be used *in vivo*.

In vitro and in vivo CT/MRI performance of Au-TEMPO NRs

In this work, Au-TEMPO NRs are supposed to be used as dual-mode CT/MRI agents because Au NPs have long been studied as enhanced contrast agents for CT measurement, and nitroxides have been applied as T₁-weighted MRI contrast agents. Thus, an *in vitro* CT measurement was conducted. A series of Au-TEMPO NRs solutions ([Au]=95, 188,

375, 750, 1,500, and 3,000 $\mu\text{g/mL}$ in PBS solution) were accurately prepared, and the concentrations of Au were analyzed by ICP-OES. A clinically used iodine contrast agent (Iodixanol) was selected as a positive control to investigate the *in vitro* CT imaging ability of Au-TEMPO NRs. In Figure 4A, Au-TEMPO NRs show a concentration-dependent CT enhancement and a linear relationship can be found between the HU value (CT signal intensity) and the concentration of Au in Au-TEMPO NRs solution from 95 $\mu\text{g/mL}$ to 3,000 $\mu\text{g/mL}$ as well as with iodine in clinical iodixanol. It can be clearly observed that Au-TEMPO NRs had stronger CT-enhancing ability than that of iodixanol at the same concentration. Higher HU values were seen on representative CT images obtained from Au-TEMPO NRs than that of iodixanol with the same concentration of Au and iodine. These data clearly indicated that Au-TEMPO NRs had good CT enhancement. At the same time, an *in vitro* MRI experiment was studied to evaluate the T₁-weighted MRI enhancement of Au-TEMPO NRs. A clinical Gd-DTPA solution was used as a reference to compare the T₁ enhancement effect between Gd-DTPA and Au-TEMPO NRs with the same concentration (Figure 4B). Clearly, Au-TEMPO NRs show a better contrast enhancement effect than clinical Gd-DTPA.

Next, we conducted the *in vivo* animal experiment to verify the possibility of these Au-TEMPO NRs being used as dual-mode contrast agents for CT/MRI measurement to diagnose tumors. For the *in vivo* study, 4T1 cells (5×10^6 cells per mouse) were injected subcutaneously into the right armpit of the mice. After 4 weeks, when the tumor volume reached approximately 0.2 cm^3 , 0.1 mL Au-TEMPO NRs solution (1,000 $\mu\text{g/mL}$) was injected as a contrast agent into the tumor. Both the *in vivo* CT/MRI images were gathered at 0, 5, and

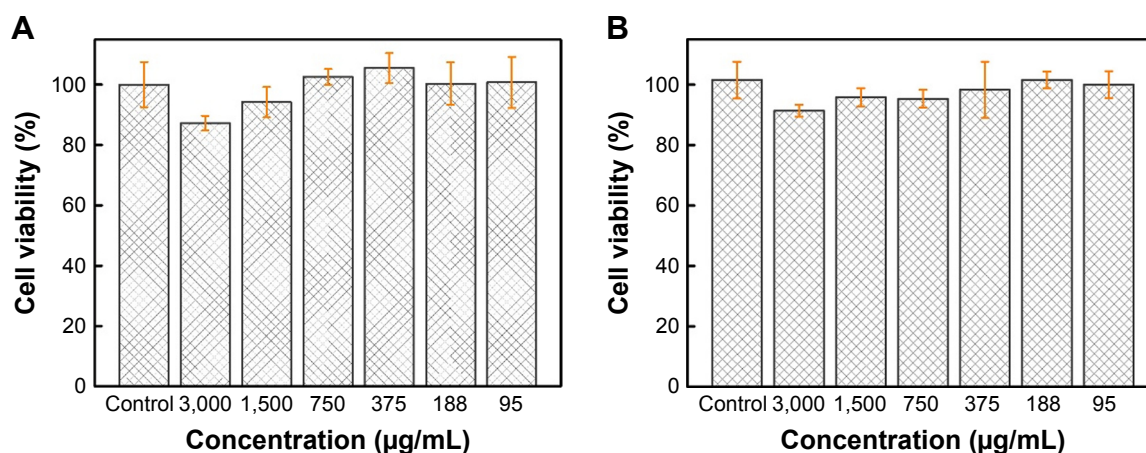


Figure 3 Cytotoxicity profiles of 4T1 cells (A) and HUVECs (B) post 12-hour incubation with Au-TEMPO NRs solution with different Au concentrations by using MTT assay. **Abbreviations:** Au-TEMPO NRs, nitroxide-radicals-modified gold nanorods; HUVEC, human umbilical vein endothelial cells.

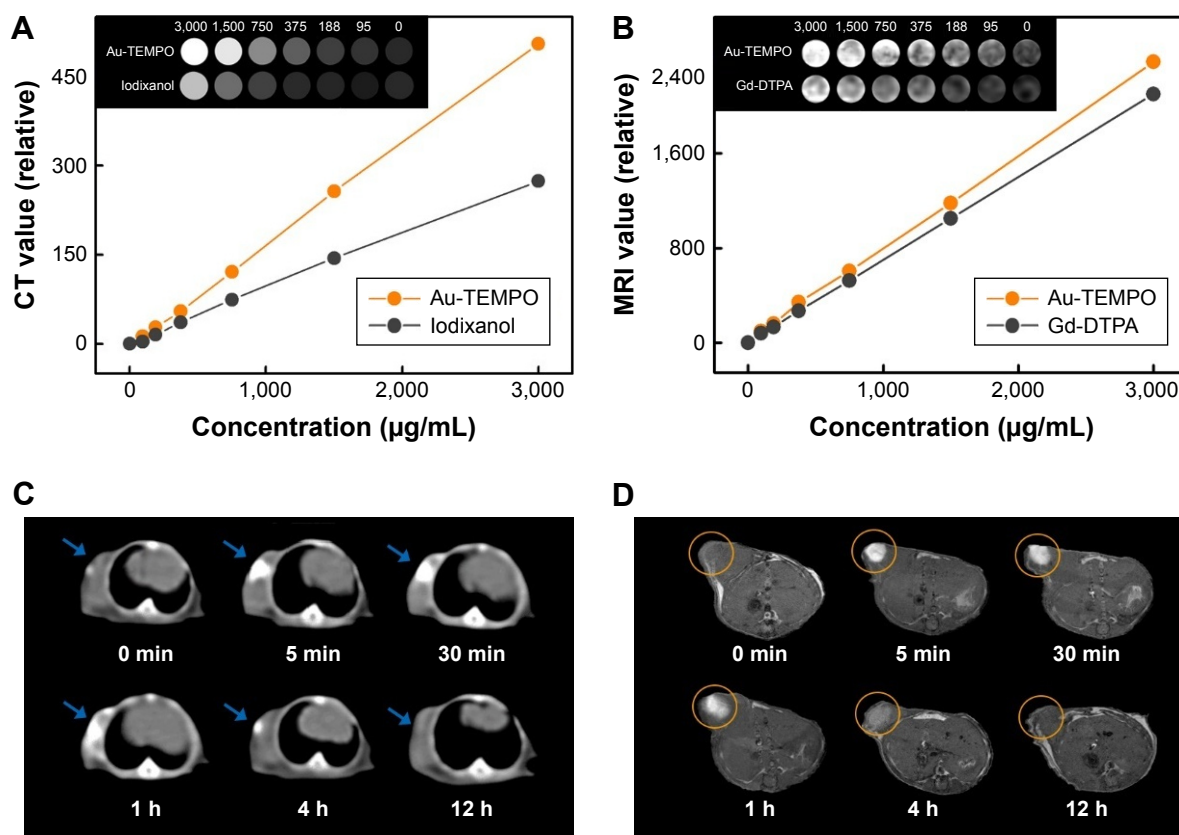


Figure 4 (A) CT images and HU values of Au-TEMPO NRs and iodixanol solutions. (B) MR images and T1 signals of Au-TEMPO NRs and Gd-DTPA solutions. (C) CT and (D) T1-weighted MR images of tumor after orthotopic injection of Au-TEMPO NRs in female BALB/c mice for 0–12 hours.

Abbreviation: Au-TEMPO NRs, nitroxide-radicals–modified gold nanorods.

30 minutes and 1, 4, and 12 hours after injection. In vivo CT imaging was assessed using a clinical CT scanner. As shown in Figure 4C, bright white areas could be clearly observed in the tumor area after orthotopic injection. Although the brightness would decrease with time extension due to metabolism and diffusion of Au-TEMPO NRs, a relatively obvious contrast enhancement could be maintained at least 4 hours after injection, which provided a longer period for diagnosis. Meanwhile, in vivo MR imaging was conducted on female BALB/c mice using a 7.0 T animal MRI scanner (Figure 4D). The T1 signal in the tumor area enhanced immediately after injection, and the obvious bright zone could exist for 4 hours; this was consistent with the conclusions of the in vivo CT study.

In vitro photothermal irradiation

As Au nanorods have been widely applied in the photothermal cancer therapy, the photothermal ability of Au-TEMPO NRs was tested. A solution of Au-TEMPO NRs (1,000 $\mu\text{g/mL}$) was irradiated by 808-nm laser for 15 minutes in order to study the photothermal effect of Au-TEMPO NRs. In Figure 5A, the heating rate of the Au-TEMPO

NRs solution was obviously higher than that of pure water, rapidly exceeded 40°C in 5 minutes, and finally rose to 50°C under laser irradiation, which was sufficiently high to cause damage to the cell membrane and resulted in cell death. The photothermal effect of Au-TEMPO NRs on cancer cells was assessed with an MTT assay to check the cell viability after irradiation. Sterilized Au-TEMPO NRs were added to DMEM to prepare a series of cell culture media of various concentrations, and 4T1 cells were cultured in these media for 4 hours, followed by laser irradiation. From Figure 5B, it is clearly seen that without the aid of Au-TEMPO NRs, there was no cytotoxicity observed in 4T1 cells even after the laser irradiation (Figure 5B). After the incubation with Au-TEMPO NRs, the cell viability decreased upon the increased concentration of Au-TEMPO NRs. The cell mortality rate reached 73.87% when Au concentration increased to 3,000 $\mu\text{g/mL}$ after laser irradiation.

Furthermore, the photothermal cancer therapeutic ability of Au-TEMPO NRs against cancer cells was evaluated through flow cytometry. After 4T1 cells were incubated with Au-TEMPO NRs for 12 hours, followed by laser irradiation, these cells were subjected to an Annexin V–FITC/

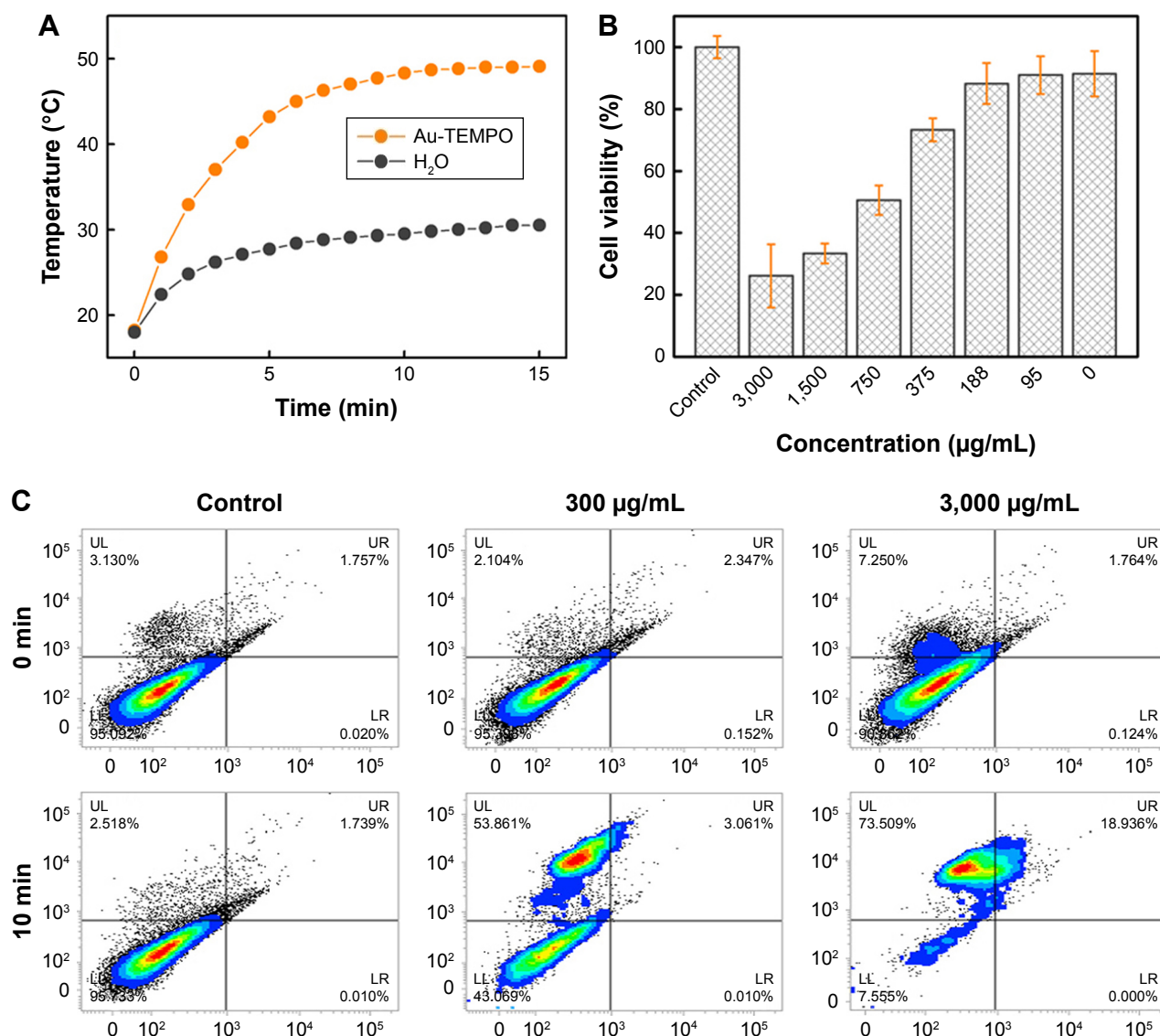


Figure 5 (A) Temperature–time curves of laser-irradiated Au-TEMPO NRs solution and PBS ([Au]=1,000 μg/mL, laser: 808 nm, 1.13 W/cm²). (B) Cell viability of 4T1 cells irradiated with 808-nm laser for 15 minutes with different concentrations of Au-TEMPO NRs via MTT assay. (C) Apoptotic analysis of 4T1 cells after 12 hours of treatment of NPs with Annexin V-FITC/PI staining.

Abbreviation: Au-TEMPO NRs, nitroxide-radicals–modified gold nanorods.

PI double-staining assay against 4T1 cells to measure cell viability by using flow cytometry (Figure 5C). For the control group without the Au-TEMPO NRs, the apoptosis of 4T1 cells did change much from before to after the laser irradiation. When incubated with 300 μg/mL Au-TEMPO NRs, the apoptosis rate of 4T1 cells reached 53.9% after laser irradiation – higher than that noted pre-irradiation. The apoptosis rate continued to rise to 73.5% when cells were incubated with 3,000 μg/mL of Au-TEMPO NRs. All of these data clearly indicated that Au-TEMPO NRs possess good photothermal ability and have the potential to be used in cancer therapy.

Fluorescence microscopy could directly provide information pertaining to cells treated with Au-TEMPO NRs and

laser irradiation. After being co-cultured with Au-TEMPO NRs and laser irradiation, these 4T1 cells were stained with a Calcein-AM/PI Kit and observed under a fluorescence microscope (Figure 6). For the control group (without the Au-TEMPO NRs), after laser irradiation, almost no red color (cell stained with PI) was seen in the image, indicating that there were almost no apoptotic cells. However, when 4T1 cells were incubated with Au-TEMPO NRs, after irradiation, many red spots were clearly observed in the image, demonstrating that 4T1 cells were killed after this combined treatment. Furthermore, a higher dose of Au-TEMPO NRs would result in a higher cell apoptosis rate. Collectively, this fluorescence measurement confirmed that Au-TEMPO NRs had good photothermal conversion ability.

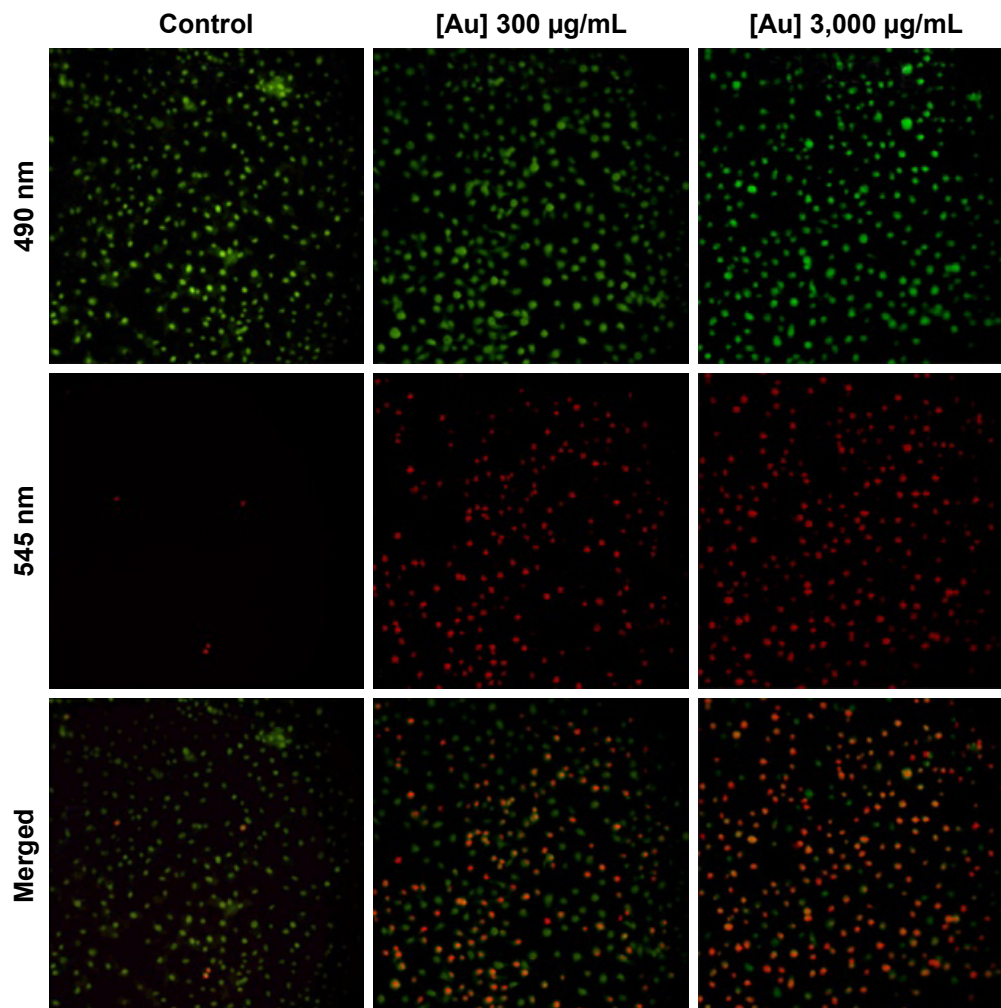


Figure 6 Fluorescence images of 4T1 cells which underwent laser irradiation post the Au-TEMPO NRs incubation.

Abbreviation: Au-TEMPO NRs, nitroxide-radicals–modified gold nanorods.

Bio-distribution and histological study

The bio-distribution and retention time are two important factors that influence the fate of NPs in vivo. Thus, the in vivo circulation and tissue distribution of Au-TEMPO NRs were studied. The amounts of Au ions in blood, heart, liver, spleen, lung, and kidney of mice after injection at

different time points (0, 1, 4, 8, 12, 24, and 48 hours) were measured by ICP-OES (Figure 7A). The Au concentration in blood rapidly increased 1 hour post injection and then gradually decreased, whereas the concentration in the liver and spleen continued to rise, because the Au-TEMPO NRs in blood were gradually taken up by the liver and spleen

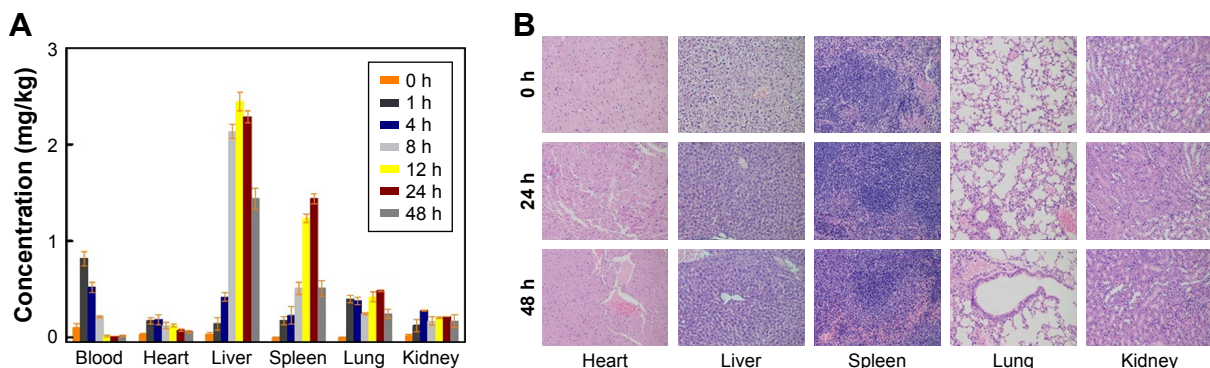


Figure 7 (A) In vivo bio-distribution (blood, heart, liver, spleen, lung, and kidney) studies of the Au-TEMPO NRs (0, 1, 4, 8, 12, 24, and 48 hours after injection). (B) Representative pathological images of main organs (heart, liver, spleen, lung, and kidney at 0, 24, and 48 hours after injection) after H&E staining.

Abbreviation: Au-TEMPO NRs, nitroxide-radicals–modified gold nanorods.

from circulation. According to the literature, the retention time *in vivo* was affected by the size and surface properties of nanomedicine. The proper increase of particle size and surface modification of PEG lead to a long retention time *in vivo*.^{36,37} In this work, the size of Au-TEMPO NRs was approximately 40 nm, which was large enough to ensure their longer retention in the blood when they were injected *in vivo*. Furthermore, the surface of these Au-TEMPO NRs was modified with mPEG, which greatly screens the interaction between Au-TEMPO NRs and biomolecules (such as proteins), thereby further increasing their retention time in the blood. Collectively, these Au NRs have a long retention time in blood and will accumulate at the tumor site due to the enhanced permeability and retention effect.

Therefore, these Au-TEMPO NRs can stay a longer time in the blood compared to the small molecular imaging agents and could passively aggregate in the liver and spleen. H&E staining of main organs (heart, liver, spleen, lung, and kidney)

sections from normal mice was conducted to study the histological toxicity of Au-TEMPO NRs. As shown in Figure 7B, almost no necrotic or apoptotic cells, histological abnormalities, or inflammatory lesions were observed in all organ tissues, indicating that Au-TEMPO NRs might not cause damage to normal cells and thus signifying their good biocompatibility.

In vivo antitumor effect

Subsequently, the *in vivo* antitumor effect of these Au-TEMPO NRs under laser irradiation was evaluated on a 4T1-tumor-bearing mouse model. Tumor mice which received the treatments of PBS and Au-TEMPO NRs without laser irradiation did not show obvious suppression in tumor growth (Figure 8A). The tumor volume reached approximately 15-fold for the PBS group and 12.5-fold for Au-TEMPO NRs, respectively, on Day 30 post the treatment compared with the original size. However, for the mice receiving the combined

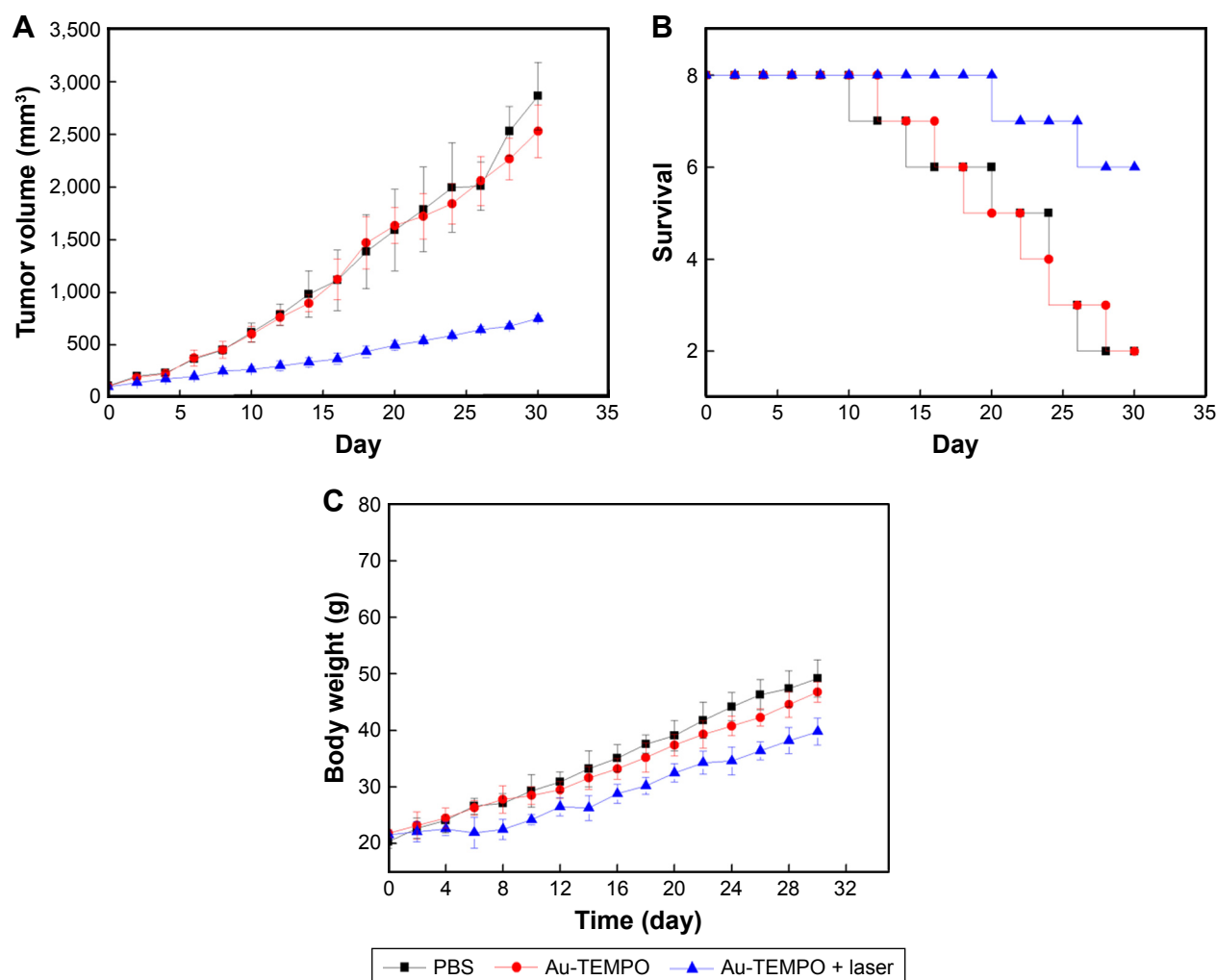


Figure 8 (A) Tumor volumes; (B) survival curves; and (C) body weight of 4T1 tumor-bearing mice received different treatments. Laser: 808 nm, 1.13 W/cm². Data are expressed as the mean \pm SD (n=8).

Abbreviation: Au-TEMPO NRs, nitroxide-radicals-modified gold nanorods.

treatment of Au-TEMPO NRs and laser irradiation, the tumor grew slowly and its size was only 3.5-fold on Day 30 when compared to that of the first day. These results clearly demonstrated that, with the laser irradiation, Au-TEMPO NRs can significantly suppress the tumor because of the photothermal effect. Moreover, the survival of these tumor-bearing mice was studied (Figure 8B). Mice treated with Au-TEMPO and laser irradiation had the highest survival rate. There were six mice alive at the end of the experiment (on Day 30), whereas only two mice were alive on Day 30 in both the PBS- and Au-TEMPO NRs-treated groups. We found that no obvious changes (body weight lost) in the body weight of the mice were observed during the course of the study for all groups, implying that Au-TEMPO NRs displayed no obvious acute toxicity (Figure 8C). Collectively, the *in vivo* antitumor experiment proved that, with the laser irradiation, Au-TEMPO NRs displayed remarkable antitumor ability.

Conclusion

In summary, we successfully synthesized a CT/MRI dual-contrast agent by conjugating 4-amino-TEMPO to Au NRs. In the given concentration range, these Au-TEMPO NRs have good biocompatibility, water solubility, and longer blood circulation time and could be stored at low temperatures for at least 1 month. Moreover, they showed a relatively high-contrast ability for CT/MRI measurement. Upon laser irradiation, the proliferation of solid tumor was greatly suppressed. These primary research results indicated that the Au-TEMPO NRs might play an important role in future clinical diagnosis and treatment of cancer with high accuracy and sensitivity.

Acknowledgments

This work was supported by the National Science and Technology Major Project (grant no 2017YFA0205400), the National Natural Science Foundation of China (grant nos 21474047 and 51773089), the Natural Science Foundation of Jiangsu Province (Grant no BK20181204), the Jiangsu Provincial Medical Youth Talent (grant no QNRC2016039), and the Technique Development Foundation of Nanjing (Outstanding Youth Foundation; grant no JQX15004).

Disclosure

The authors report no conflicts of interest in this work.

References

1. Sun IC, Eun DK, Koo H, et al. Tumor-targeting gold particles for dual computed tomography/optical cancer imaging. *Angew Chem Int Ed Engl*. 2011;50(40):9520–9523.
2. Gussoni M, Greco F, Ferruti P, et al. Poly(amidoamine)s carrying TEMPO residues for NMR imaging applications. *New J Chem*. 2008; 32(2):323–332.
3. Chen Q, Li K, Wen S, et al. Targeted CT/MR dual mode imaging of tumors using multifunctional dendrimer-entrapped gold nanoparticles. *Biomaterials*. 2013;34(21):5200–5209.
4. Wang L, Xing H, Zhang S, et al. A Gd-doped Mg-Al-LDH/Au nanocomposite for CT/MR bimodal imaging and simultaneous drug delivery. *Biomaterials*. 2013;34(13):3390–3401.
5. Litti L, Rivato N, Fracasso G, et al. A SERRS/MRI multimodal contrast agent based on naked Au nanoparticles functionalized with a Gd(III) loaded PEG polymer for tumor imaging and localized hyperthermia. *Nanoscale*. 2018;10(3):1272–1278.
6. Teramoto A, Fujita H, Yamamuro O, Tamaki T. Automated detection of pulmonary nodules in PET/CT images: Ensemble false-positive reduction using a convolutional neural network technique. *Med Phys*. 2016;43(6):2821–2827.
7. Jadvar H, Colletti PM. Competitive advantage of PET/MRI. *Eur J Radiol*. 2014;83(1):84–94.
8. Zhang C, Ren J, Hua J, et al. Multifunctional Bi₂WO₆ Nanoparticles for CT-Guided Photothermal and Oxygen-free Photodynamic Therapy. *ACS Appl Mater Interfaces*. 2018;10(1):1132–1146.
9. Liu S, Li H, Xia L, et al. Anti-RhoJ antibody functionalized Au@I nanoparticles as CT-guided tumor vessel-targeting radiosensitizers in patient-derived tumor xenograft model. *Biomaterials*. 2017;141:1–12.
10. Huo D, Liu S, Zhang C, et al. Hypoxia-Targeting, Tumor Microenvironment Responsive Nanocluster Bomb for Radical-Enhanced Radiotherapy. *ACS Nano*. 2017;11(10):10159–10174.
11. McClellan BL, Preston M. Hickey memorial lecture. Ionic and nonionic iodinated contrast media: evolution and strategies for use. *AJR Am J Roentgenol*. 1990;155(2):225–233.
12. Saito K, Kotake F, Ito N, et al. Gd-EOB-DTPA enhanced MRI for hepatocellular carcinoma: quantitative evaluation of tumor enhancement in hepatobiliary phase. *Magn Reson Med Sci*. 2005;4(1):1–9.
13. Rammohan N, Holbrook RJ, Rotz MW, et al. Gd(III)-Gold Nanoconjugates Provide Remarkable Cell Labeling for High Field Magnetic Resonance Imaging. *Bioconjug Chem*. 2017;28(1):153–160.
14. Yu X, Wadghiri YZ, Sanes DH, Turnbull DH. In vivo auditory brain mapping in mice with Mn-enhanced MRI. *Nat Neurosci*. 2005;8(7):961–968.
15. Haedicke IE, Li T, Zhu YLK, et al. An enzyme-activatable and cell-permeable Mn III-porphyrin as a highly efficient T₁ MRI contrast agent for cell labeling. *Chem Sci*. 2016;7(7):4308–4317.
16. Zhu H, Zhang L, Liu Y, et al. Aptamer-PEG-modified Fe₃O₄@Mn as a novel T1- and T2-dual-model MRI contrast agent targeting hypoxia-induced cancer stem cells. *Sci Rep*. 2016;6:39245.
17. Yuan Y, Ding Z, Qian J, et al. Casp3/7-Instructed Intracellular Aggregation of Fe₃O₄ Nanoparticles Enhances T2 MR Imaging of Tumor Apoptosis. *Nano Lett*. 2016;16(4):2686–2691.
18. Ferrucci JT. Advances in abdominal MR imaging. *Radiographics*. 1998;18(6):1569–1586.
19. Xu Z, Hou Y, Sun S. Magnetic core/shell Fe₃O₄/Au and Fe₃O₄/Au/Ag nanoparticles with tunable plasmonic properties. *J Am Chem Soc*. 2007; 129(28):8698–8699.
20. Pan CT, Shen SC. Magnetically actuated bi-directional microactuators with permalloy and Fe/Pt hard magnet. *J Magn Magn Mater*. 2005;285(3):422–432.
21. Marckmann P, Skov L, Rossen K, et al. Nephrogenic systemic fibrosis: suspected causative role of gadodiamide used for contrast-enhanced magnetic resonance imaging. *J Am Soc Nephrol*. 2006;17(9):2359–2362.
22. Quintessenz Verlagsgmbh NMO. Multi-modal volume registration of the Temporo-mandibular joint by using MRI- and CT-imagery. *Int Poster J Dent Oral Med*. 2000;4:50.
23. Huang X, Neretina S, El-Sayed MA. Gold nanorods: from synthesis and properties to biological and biomedical applications. *Adv Mater*. 2009;21(48):4880–4910.
24. Guo J, Rahme K, He Y, et al. Gold nanoparticles enlighten the future of cancer theranostics. *Int J Nanomedicine*. 2017;12:6131–6152.

25. Zhang S, Li Y, He X, et al. Photothermalysis mediated by gold nanorods modified with EGFR monoclonal antibody induces Hep-2 cells apoptosis in vitro and in vivo. *Int J Nanomedicine*. 2014;9:1931–1946.
26. Qu X, Qiu P, Zhu Y, Yang M, Mao C. Guiding nanomaterials to tumors for breast cancer precision medicine: from tumor-targeting small-molecule discovery to targeted nanodrug delivery. *NPG Asia Mater*. 2017;9:e452.
27. Hayashi H, Ohkubo K, Karasawa S, Koga N. Assemblies of functional small-sized molecules having 4-amino-2,2,6,6-tetramethylpiperidine-1-oxyl responsive to heat and pH in water and their water proton relaxivities. *Langmuir*. 2011;27(20):12709–12719.
28. Achadu OJ, Britton J, Nyokong T. Graphene Quantum Dots Functionalized with 4-Amino-2, 2, 6, 6-Tetramethylpiperidine-N-Oxide as Fluorescence “Turn-ON” Nanosensors. *J Fluoresc*. 2016;26(6): 2199–2212.
29. Rajca A, Wang Y, Boska M, et al. Organic radical contrast agents for magnetic resonance imaging. *J Am Chem Soc*. 2012;134(38): 15724–15727.
30. Hyodo F, Matsumoto K, Matsumoto A, Mitchell JB, Krishna MC. Probing the intracellular redox status of tumors with magnetic resonance imaging and redox-sensitive contrast agents. *Cancer Res*. 2006;66(20): 9921–9928.
31. Niidome T, Yamagata M, Okamoto Y, et al. PEG-modified gold nanorods with a stealth character for in vivo applications. *J Control Release*. 2006;114(3):343–347.
32. Maurel V, Laferrière M, Billone P, Godin R, Scaiano JC. Free radical sensor based on CdSe quantum dots with added 4-amino-2,2,6,6-tetramethylpiperidine oxide functionality. *J Phys Chem B*. 2006;110(33): 16353–16358.
33. And BN, Elsayed MA. Preparation and growth mechanism of gold nanorods (NRs) using seed-mediated growth method. *Chemistry of Materials*. 2003;15(10):1957–1962.
34. Guo R, Zhang L, Qian H, et al. Multifunctional nanocarriers for cell imaging, drug delivery, and near-IR photothermal therapy. *Langmuir*. 2010;26(8):5428–5434.
35. Audran G, Bosco L, Brémond P, et al. Enzymatically Shifting Nitroxides for EPR Spectroscopy and Overhauser-Enhanced Magnetic Resonance Imaging. *Angew Chem Int Ed Engl*. 2015;54(45):13379–13384.
36. Liu Z, Davis C, Cai W, He L, Chen X, Dai H. Circulation and long-term fate of functionalized, biocompatible single-walled carbon nanotubes in mice probed by Raman spectroscopy. *Proc Natl Acad Sci U S A*. 2008; 105(5):1410–1415.
37. Gref R, Lück M, Quéllec P, et al. “Stealth” corona-core nanoparticles surface modified by polyethylene glycol (PEG): influences of the corona (PEG chain length and surface density) and of the core composition on phagocytic uptake and plasma protein adsorption. *Colloids Surf B Biointerfaces*. 2000;18(3–4):301–313.

International Journal of Nanomedicine

Publish your work in this journal

The International Journal of Nanomedicine is an international, peer-reviewed journal focusing on the application of nanotechnology in diagnostics, therapeutics, and drug delivery systems throughout the biomedical field. This journal is indexed on PubMed Central, MedLine, CAS, SciSearch®, Current Contents®/Clinical Medicine,

Submit your manuscript here: <http://www.dovepress.com/international-journal-of-nanomedicine-journal>

Dovepress

Journal Citation Reports/Science Edition, EMBASE, Scopus and the Elsevier Bibliographic databases. The manuscript management system is completely online and includes a very quick and fair peer-review system, which is all easy to use. Visit <http://www.dovepress.com/testimonials.php> to read real quotes from published authors.